# The Structure−Activity Relationship of Ferric Pyoverdine Bound to Its Outer Membrane Transporter: Implications for the Mechanism of Iron Uptake[†]

V. Schons,[‡] R. A. Atkinson,[§] C. Dugave,[||] R. Graff,[⊥] G. L. A. Mislin,[‡] L. Rochet,[‡] C. Hennard,[‡] B. Kieffer,[§] M. A. Abdallah,[‡] and I. J. Schalk*,[‡]

*UMR7100 CNRS, ESBS, Bld Sébastien Brant, F-67 412 Illkirch, Strasbourg, France, Laboratoire de Biologie et de Genomique Structurales, UMR 7104, ESBS, Bld Sébastien Brant, F-67 412 Illkirch, Strasbourg, France, CEA/Saclay, Département d'Ingénierie et d'Etudes des Protéines, Bâtiment 152, F-91191 Gif sur Yvette, France, and Service Commun de RMN, Faculté de Chimie, ULP, 1 rue Blaise Pascal, 67008, Strasbourg Cedex, France*

*Received June 15, 2005; Revised Manuscript Received September 2, 2005*

ABSTRACT: Under iron limitation, *Pseudomonas aeruginosa* ATCC 15692 secretes a major siderophore, pyoverdine I (PvdI). This molecule chelates iron in the extracellular medium and shuttles it into the cells via a specific outer membrane transporter, FpvAI. PvdI consists of a fluorescent chromophore derived from 2,3-diamino-6,7-dihydroxyquinoline and containing one of the bidentate groups involved in iron chelation, linked to a peptide moiety containing the two other bidentate groups required for binding to $Fe^{3+}$. Kinetic studies, based on the fluorescence properties of this siderophore, showed that pH 8.0 was optimal for the binding of PvdI and PvdI-Fe to FpvAI. We investigated the mechanism of interaction of PvdI and PvdI-Fe with FpvAI, by synthesizing various analogues of this siderophore, determining their affinity for FpvAI in vitro and in vivo and their ability to transport iron, and interpreting the results obtained in light of the structure of FpvAI−PvdI. Our findings demonstrate that the succinyl moiety linked to the chromophore of PvdI and the first amino acid of the peptide moiety can be sterically hindered with no effect on binding or the iron uptake properties of PvdI-Fe. Moreover, the sequence and the structure of the peptide moiety of PvdI seems to be more important for the iron uptake step than for the binding of the siderophore to FpvAI. Finally, the efficiency of iron uptake and of recycling of the various PvdI analogues after iron release suggests that iron dissociates from PvdI on FpvAI or in the periplasm. All these data have serious implications for the specificity and mechanism of PvdI-mediated iron transport in *P. aeruginosa*.

Most bacteria meet their iron requirements by producing and secreting low-molecular mass, iron-binding compounds called siderophores. Siderophores provide the cell with iron by solubilizing the ferric ion, which otherwise tends to form insoluble complexes, in aerobic conditions and at physiological pH. The uptake of ferric-siderophores into gram-negative bacteria involves a specific outer membrane transporter (OMT) and an inner membrane ABC transporter (*1*, *2*). The energy required for transport across the inner membrane is provided by ATP hydrolysis. The proton motive force of the inner membrane drives OMT-mediated transport across the outer membrane by means of an inner membrane complex comprising TonB, ExbB, and ExbD (*3*, *4*).

Under conditions of iron limitation, fluorescent *Pseudomonas* strains produce yellow-green, water-soluble siderophores called pyoverdines (Pvd).[1] More than 100 different Pvds have been identified (personal communication from Dr J.-M. Meyer). They form a wide class of mixed siderophores, composed of a chromophore derived from 2,3-diamino-6,7-dihydroxyquinoline linked to a peptide, differing considerably from one Pvd to another, in terms of both the number and nature of the amino acids (*5*, *6*). The structures of three different Pvd−metal complexes have been described and shown to differ completely, depending on the peptide moiety (*7*−*9*).

Iron uptake via the Pvd pathway in fluorescent *Pseudomonas* strains is highly strain-specific, implying that the bacteria are able to incorporate the iron complexes of their own Pvd, but cannot use those of structurally different exogenous Pvds (*5*, *10*−*12*). This is due to highly specific recognition of the cognate siderophore by the OMT. The recognition mechanism probably involves the peptide moiety of the Pvd molecule. However, heterologous uptake may occur if Pvds contain peptides with similar sequences, as is the case for *Pseudomonas aeruginosa* ATCC 15692 and *Pseudomonas*

[†] This work was funded by the Centre National de la Recherche Scientifique (Programme Physique et Chimie du Vivant), the Ministère de l'Enseignement Supérieur, de la Recherche et de la Technologie (ACC-SDV5) and the association Vaincre la Mucoviscidose.

* To whom correspondence should be addressed. E-mail: schalk@esbs.u-strasbg.fr. Phone: (+33) (0) 3 90 24 47 19. Fax: (+33) (0) 3 90 24 48 29.

[‡] UMR7100 CNRS, ESBS.

[§] UMR 7104, ESBS.

[||] CEA/Saclay.

[⊥] Faculté de Chimie, ULP.

[1] Abbreviations: PvdI and PvdI-Fe, iron-free and ferric pyoverdine, respectively, produced by *Pseudomonas aeruginosa 15692*; apo-Pflu and Pflu-Fe, iron-free and iron-loaded pyoverdine, respectively, produced by *Pseudomonas fluorescens 13555*; FpvAI, PvdI outer membrane receptor; HPLC, high-performance liquid chromatography; FRET, fluorescence resonance energy transfer.

10.1021/bi051155s CCC: $30.25 
Published on Web 10/05/2005

*fluorescens* ATCC 13525 (*5*, *13*). For *P. aeruginosa* strains, three structurally different Pvds (PvdI, II, and III) have been identified, each recognized at the outer membrane by a specific transporter (*14*). The PvdI receptor (*fpvAI*), the best-characterized Pvd OMT, was cloned by Poole et al. in 1993 (*15*), and its structure was solved in 2005 (*16*). The genes encoding the receptors for PvdII and PvdIII, *fpvAII* and *fpvAIII*, were also recently identified (*17*). Finally, an additional receptor, FpvB, which takes up PvdI, has been identified, and its presence has been demonstrated in several *P. aeruginosa* strains (*18*).

The biochemical properties of FpvAI have been studied in our laboratory using the fluorescent properties of PvdI. Iron-free PvdI has spectral properties suitable for FRET with the Trp residues of FpvAI (*19*). When this technique was used, it was shown that, under iron-deficient conditions, the normal state of this transporter is the FpvAI−PvdI complex (*16*, *19*, *20*). FpvAI is able to bind PvdI and PvdI-Fe with similar affinities but different kinetics, at a common binding site (*19*−*22*). The FpvAI−PvdI complex forms much more slowly than the FpvAI−PvdI-metal complex (*22*), but both PvdI and PvdI-metal adsorb to FpvAI with biphasic kinetics and two apparent association rate constants ($k_{app1}$ and $k_{app2}$): the bimolecular step (association of the ligand with the receptor) is followed by a slower step that presumably leads to a more stable complex (*22*). The most likely explanation for this second step is that the binding of the ligand to the receptor induces a conformational change on FpvAI, which may differ with the loading status (metal-loaded or metal-free) of PvdI.

FpvAI (*16*), like FptA (*23*), FhuA (*24*, *25*), FepA (*26*), and FecA (*27*, *28*)—the outer membrane transporters (OMT) of pyochelin in *P. aeruginosa* and of ferrichrome, ferric-enterobactin and ferric-citrate in *Escherichia coli*, respectively,—consists of a C-terminal $\beta$-barrel domain and an N-terminal plug domain filling the barrel. The binding site for the ferric siderophore is located above the cork, well outside the membrane, and is composed of residues of the plug and $\beta$-barrel domains (*16*). The electrostatic properties of the siderophore-binding pocket are specific to each OMT and depend on the chemical features of the siderophore. The binding pocket of iron-free PvdI on FpvAI consists mostly of aromatic residues, with six Tyr residues, two Trp residues, and only three hydrophilic residues (*16*). In the FhuA−ferrichrome structure (*24*, *25*), eight aromatic and two hydrophilic residues form the ferrichrome binding site. The ferric citrate binding pocket of FecA consists of five Arg residues that interact with the negatively charged ferric citrate (*27*, *28*).

The structure of FpvAI−PvdI has been solved, but many questions remain concerning the mechanisms by which PvdI-Fe interacts with FpvAI during iron uptake. In the present work, we address some of these questions, using various techniques. We investigated the effect of pH on the kinetics of binding of PvdI and PvdI−Ga to FpvAI. We synthesized several photoactivatable analogues of PvdI and investigated their affinity for FpvAI and their ability to transport iron. We found that PvdI and PvdI-Fe bound to FpvA by means of similar mechanisms. Finally, the efficiency with which the PvdI analogues on FpvAI were recycled following iron release suggests that iron dissociates from PvdI on FpvAI or in the periplasm.

## MATERIALS AND METHODS

*Chemicals.* We obtained 4-azidobenzoic acid *N*-hydrosuccinimide ester and triethylamine from Sigma (Saint Quentin Fallavier, France). Octyl-POE (*N*-octyl-polyoxyethylene) was purchased from Bachem (Basel, Switzerland). $^{55}FeCl_3$ and succinimidyl 4-azidobenzoate, *N*-[benzoate-3,5-$^3$H] were obtained from NEN (Boston, MA).

*Growth Conditions and Purification of FpvAI, PvdI-Fe, and Pflu-Fe.* The strains used in this study were the wild-type strain *P. aeruginosa* ATCC 15692 and two mutants: CDC5(pPVR2), which overproduces FpvAI and is PvdI-deficient, and K691(pPVR2) (*29*), which overproduces FpvAI and produces PvdI (*15*).

PvdI-Fe (*30*, *31*) and Pflu-Fe (*32*) were prepared as described previously. PvdI and Pflu concentrations were determined spectrophotometrically, using the molar extinction coefficient of $\epsilon_{380\ nm} = 16\ 500\ M^{-1}$ and $\epsilon_{400\ nm} = 19\ 000\ M^{-1}$ for the iron-free and ferric-loaded PvdI and Pflu forms (*31*, *33*).

*Synthesis of PvdI-Fe Analogues. 1. Synthesis of $N_3$-Ser−PvdI-Fe.* We dissolved 30 mg (20 mmol) of PvdI-Fe in 100 $\mu$L of a mixture of dimethylformamide−water (7:1). We then added 3 $\mu$L of triethylamine and 15.6 mg (60 mmol) of 4-azidobenzoic acid *N*-hydrosuccinimide ester dissolved in 200 $\mu$L of dimethylformamide−water (7:1). The formation of $N_3$-Ser−PvdI-Fe was followed by electrophoretic analysis on cellulose acetate membranes (Midifilm, Biomidi), in a horizontal electrophoresis tank containing 100 mM pyridine−acetic acid, pH 5.0, at a constant voltage (300 V) for 30 min (*34*). The mixture was left to stand for 2 h at room temperature and was then purified by HPLC on a $C_{18}$ column (10 mm particle size C-18 nucleosil from Macherey-Nagel as the bonded phase, 250 mm × 25 mm). The eluent was 200 mM pyridine−acetic acid, pH 5.0/$CH_3CN$ (18%), at a flow rate of 8 mL/min. We obtained 19.5 mg of $N_3$-Ser−PvdI-Fe (yield: 70%). Electrophoresis on cellulose acetate films (*34*) gave the following results: migration distance = 2.5 cm. FABMS: $m/z = 1479.6$ mu ($M^+$).

*2. Synthesis of Amino−PvdI-Fe.* Amino−PvdI-Fe was synthesized from PvdI-Fe as described previously (*35*).

*3. Synthesis of $N_3$-Chromo−PvdI-Fe.* $N_3$-Chromo−PvdI-Fe was prepared as described previously (*35*) from amino−Pvd-Fe and purified by HPLC as for $N_3$-Ser−PvdI-Fe (yield: 65%).

Electrophoresis on cellulose acetate films (*34*) gave the following results: migration distance = 2.8 cm. FABMS: $m/z = 1521.3$ mu ($M^+$).

*4. Synthesis of $N_3$-Lys−Pflu-Fe.* We dissolved 10 mg (8.0 mmol) of Pflu-Fe in 75 $\mu$L of a mixture of dimethylformamide−water (7:1). We then added 2 $\mu$L of triethylamine and 10 mg (38.4 mmol) of 4-azidobenzoic acid *N*-hydrosuccinimide ester dissolved in 30 $\mu$L of dimethylformamide−water (7:1). The formation of $N_3$-Lys−Pflu-Fe was monitored by electrophoresis on cellulose acetate films, as described above for the synthesis of $N_3$-Ser−PvdI-Fe. The mixture was incubated for 1 h at room temperature, and 1 mL of ethyl acetate was added. The mixture was centrifuged and the pellet dissolved in 200 $\mu$L water. Excess reagent was removed by two successive extractions with 100 $\mu$L of ethyl acetate. $N_3$-Lys−Pflu-Fe was then purified on a CM Sephadex column with 50 mM pyridine/acid acetic, pH 5.0, as

the eluent. $N_3$-Lys−Pflu-Fe was obtained with a yield of 66%. Electrophoresis on cellulose acetate films (*34*) gave the following results: migration distance = 1.3 cm. FABMS: $m/z = 1334$ mu ($M^+$).

*5. Synthesis of Tritiated [$^3$H]$N_3$-Ser−PvdI-Fe or [$^3$H]$N_3$-Chromo−PvdI-Fe.* We concentrated 45 $\mu$L (1 nmol, 45 $\mu$Ci) of a solution of succinimidyl 4-azidobenzoate, *N*-[benzoate-3,5-$^3$H] (Dupont NEN, specific activity 47 Ci/mmol) in a microfuge vial, and the residue was taken up in 10 $\mu$L of dimethylformamide−water (7:1). We then added 1.8 $\mu$g (1.2 nmol) of PvdI-Fe (for the synthesis of [$^3$H]$N_3$-Ser−PvdI-Fe**)** or $NH_2$-PvdI-Fe (for the synthesis of [$^3$H]$N_3$-Chromo−PvdI-Fe) in 11 $\mu$L of dimethylformamide−water (7:1) and 1 $\mu$L of triethylamine. The mixture was incubated for 1 h at room temperature, during which tritiated photoactivatable analogues of PvdI-Fe formed ([$^3$H]$N_3$-Ser−PvdI-Fe or [$^3$H]-$N_3$-Chromo−PvdI-Fe). These analogues were used for the photoaffinity labeling of FpvAI without further purification.

*6. Synthesis of Tritiated [$^3$H]$N_3$-Lys−Pflu-Fe.* [$^3$H]Pflu-Fe was prepared as [$^3$H]PvdI-Fe (*20*) by reduction of the α-keto carboxylic group of Pflu′-Fe (a Pflu-Fe analogue produced by *P. fluorescens* ATCC 13555 that differs from Pflu-Fe in having an α-keto carboxylic function on the succinamide group) to give an α-hydroxy acid group with tritiated sodium borohydride. Pflu′-Fe (7 mg, 5.6 $\mu$mol) was dissolved in 50 $\mu$L of sodium hydroxide solution (0.1 N) in the presence of 4 mg of sodium [$^3$H]$_4$-borohydride (11.7 Ci/mmol). The mixture was incubated for 2 h at room temperature and was then neutralized with 1 $\mu$L of acetic acid and purified by HPLC on a $C_{18}$ column (Nucleosil 250 mm × 4.5 mm). The eluent was 25 mM pyridine−acetic acid (pH 5.0)/4% (v/v) acetonitrile, at a flow rate of 0.8 mL/min. We obtained [$^3$H]Pflu-Fe with a specific activity of 3 Ci/mmol. FABMS: $m/z = 1243$ mu ($M^+$). We concentrated 350 $\mu$L (110 nmol) of [$^3$H]Pflu-Fe (specific activity 3 Ci/mmol) in a microfuge vial, and the residue was taken up in 24 $\mu$L of dimethylformamide−water (7:1). We then added 0.5 mg (1.9 $\mu$mol) of 4-azidobenzoic acid *N*-hydrosuccinimide ester in 25 $\mu$L of dimethylformamide−water (7:1) and 1 $\mu$L of triethylamine. The mixture was incubated for 1 h at room temperature, and the tritiated photoactivatable analogue of Pflu-Fe ([$^3$H]$N_3$-Lys−Pflu-Fe) was used for photoaffinity labeling without further purification.

*Decomplexation of the PvdI-Fe and Pflu-Fe Analogues.* Decomplexation of the PvdI-Fe and Pflu-Fe analogues was performed as described previously for PvdI-Fe (*34*).

*Photolysis of Azido Siderophore Analogues.* Photolysis was performed in 50 mM Tris-HCl, pH 8.0, at 29 °C, using a bench lamp emitting at 312 nm (VL-M, 6 W, Bioblock, France). The samples were kept in a quartz cell at a concentration of 25 $\mu$M and irradiated with the light source maintained at a distance of 15 cm. The visible spectrum of this solution was determined at various time points.

*$^{55}$Fe Uptake in P. aeruginosa ATCC 15692 in the Presence and Absence of Irradiation*. Iron uptake assays with the various analogues of PvdI or Pflu were carried out as previously described (*35*).

*Ligand Binding Assays.* For in vitro and in vivo competition experiments with the various PvdI-Fe or Pflu-Fe analogues, we used the filtration assay described for purified FpvAI (*19*) and that described for *P. aeruginosa* cells (*20*). These experiments were carried out in the dark for the arylazido derivatives.

*Photoaffinity Labeling of FpvAI.* We incubated 40 $\mu$L of purified FpvAI (5 nM) in 50 mM Tris-HCl, pH 7.0, and octyl POE 1% (v/v) for 20 min with 1 $\mu$M [$^3$H]$N_3$-Chromo−PvdI-Fe or [$^3$H]$N_3$-Ser−PvdI-Fe or 120 $\mu$M [$^3$H]$N_3$-Lys−Pflu-Fe. Protein solutions were irradiated for 20 min at 312 nm, with a bench lamp maintained at a distance of 8 cm. The labeled protein was analyzed by SDS−PAGE. Radioactivity was counted in slices of equal size, cut from the SDS−PAGE gel and treated as previously described (*35*). For each photoactivatable analogue, the experiment was repeated in the presence of 1 mM PvdI-Fe, used as a protective agent.

For in vivo labeling of the FpvAI receptor, CDC5(pPVR2) cells were harvested, washed with 50 mM Tris-HCl, pH 8.0, and resuspended in the same buffer at an $OD_{600}$ of 1.6. We added 1 $\mu$M [$^3$H]$N_3$-Chromo−PvdI-Fe or [$^3$H]$N_3$-Ser−PvdI-Fe or 120 $\mu$M [$^3$H]$N_3$-Lys−Pflu-Fe to 300 $\mu$L of this cell suspension. The mixtures were incubated at room temperature for 5 min and irradiated at 312 nm for 10 min, as described above. For each photoactivatable analogue, we repeated the experiment in the presence of 1 mM PvdI-Fe, used as a protective agent. The cells were disrupted by two passages through a French press cell (15 000 lb/in.$^2$). The membranes were pelleted by centrifugation at 20 000 *g* for 1 h. Outer and inner membranes were separated on a sucrose gradient (*36*), and labeling was analyzed as previously described (*35*). Periplasmic proteins were isolated from *P. aeruginosa* spheroblasts (*37*), and labeling was analyzed by SDS−PAGE.

We repeated all the in vivo and in vitro photolabeling experiments with the iron-free photoactivatable analogues ([$^3$H]$N_3$-Chromo−PvdI, [$^3$H]$N_3$-Ser−PvdI, and [$^3$H]$N_3$-Lys−Pflu). In this case, iron-free PvdI was used as the protective agent.

*Fluorescence Spectroscopy*. FRET (fluorescence resonance energy transfer) experiments were performed with a PTI (Photon Technology International TimeMaster, Bioritech) spectrofluorometer. In all experiments, the sample was stirred at 29 °C in a 1 mL cuvette, the excitation wavelength was set at 290 nm, and fluorescence emission was measured at 447 nm. We studied the kinetics of binding and iron uptake as previously described (*20*, *22*, *38*).

## RESULTS

*Effect of pH on the Stability of the Copurified FpvAI−PvdI complex*. To better understand the mechanisms by which PvdI interacts with its OMT, we studied the effect of pH on the stability of copurified FpvAI−PvdI (Figure 1A). The spectral properties of PvdI were used to monitor the presence of FpvAI−PvdI (*19*): using an excitation wavelength of 290 nm (that of Trp), fluorescence is emitted at 447 nm only if FpvAI is loaded with PvdI (*19*). We incubated copurified FpvAI−PvdI at various pH values and determined the ratio of emission at 337 nm (emission of Trp) to that at 447 nm (emission of PvdI), with excitation at 290 nm. We found that the complex was stable between pH 4 and 8.5 (emission at 337 nm/emission at 447 nm around 1; Figure 1A). Outside this range, the complex seemed to dissociate (emission at 337 nm/emission at 447 nm greater than 1).

*Effect of pH on the Binding of PvdI and PvdI-Metal.* We also investigated the binding kinetics of PvdI and PvdI−Ga

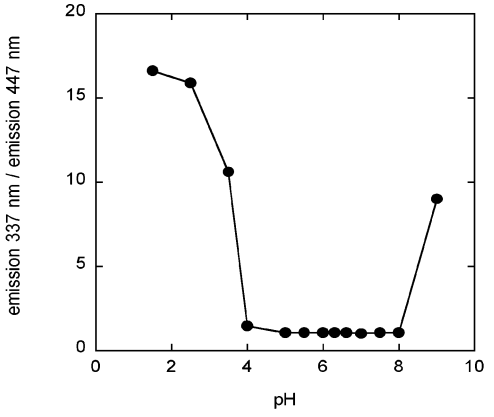


A.

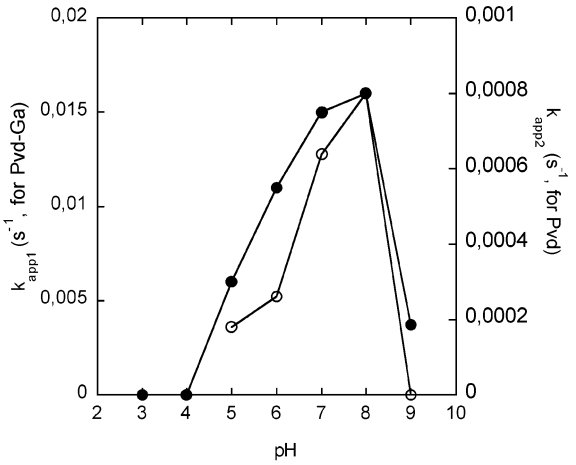


B.

FIGURE 1: (A) Effect of pH on the FpvAI−PvdI complex. The ratio of emission at 337 nm to emission at 447 nm was determined at various pH values, in 50 mM phosphate buffer. (B) Effect of pH on the PvdI and PvdI-metal binding kinetics. CDC5(pPVR2) cells were diluted in buffer at various pH values, at an $OD_{600}$ of 0.005, and incubated in the presence of 10 nM PvdI−Ga or 50 nM PvdI. Fluorescence emission was then monitored at 447 nm (excitation at 290 nm). A double exponential curve was fitted to the time course data for PvdI−Ga and a monoexponential curve was fitted for PvdI (*22*). Apparent rate constants $k_{app1}$ (for PvdI−Ga) and $k_{app2}$ (for PvdI) were plotted against pH.

as a function of pH, using FRET between PvdI and the Trp residues of FpvAI. For PvdI−Ga, we analyzed the kinetics of the binding reaction and determined the apparent association rate constants ($k_{app1}$ and $k_{app2}$) as described previously (*22*), at various pH values. Only the $k_{app1}$ value, corresponding to the first step (binding of the ligand to the transporter), was sensitive to pH (Figure 1B). For metal-free PvdI, our previous studies demonstrated a two-step binding process, but only the second step, which must be markedly slower than the first step, is visualized by FRET and occurs with a $k_{app2}$ independent of the concentration of PvdI (*22*). The first step cannot be observed either because it is too rapid or because PvdI is not close enough to a Trp residue for FRET to occur. Figure 1B shows the variation of $k_{app1}$ for PvdI−Ga and the $k_{app2}$ value for metal-free PvdI as a function of pH. Consistent with the data presented in Figure 1B, no binding was observed at pH values lower than 4.5 or higher than 9. Between pH 4.5 and pH 9, $k_{on}$ values reached a maximum at pH 8 for PvdI and PvdI−Ga.

*Synthesis of Photoactivatable Siderophore Analogues.* Photoaffinity labeling is a particularly suitable technique for investigation of the structure of receptor binding sites, for

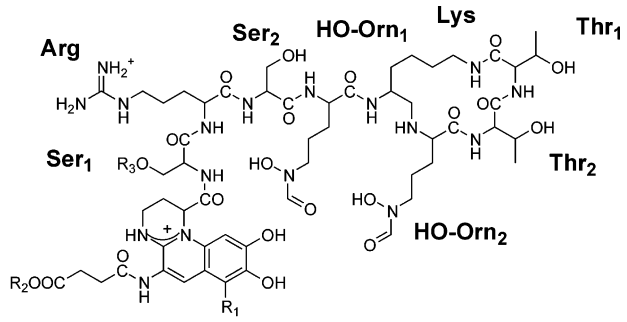


**Pvd :** $R_1$ = H; $R_2$ = H; $R_3$ = H
**$N_3$-Chromo-Pvd :** $R_1$ = H; $R_2$ = NH-$C_2H_4$-CO-$C_6H_4$-$N_3$; $R_3$ = H
**$N_3$-Ser-Pvd :** $R_1$ = H; $R_2$ = H; $R_3$ = CO-$C_6H_4$-$N_3$

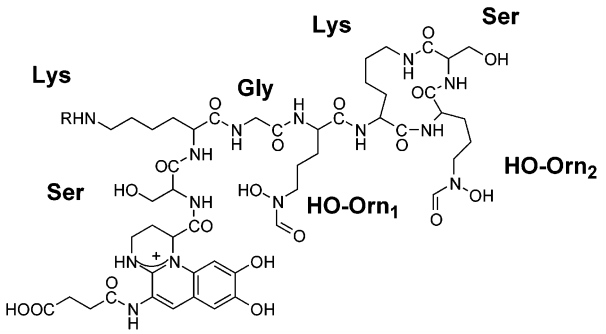


**Pflu :** R = H
**$N_3$-Lys-Pflu :** R = CO-$C_6H_4$-$N_3$

FIGURE 2: PvdI analogues and Pflu analogues.

studies of siderophore−receptor interactions during iron transport, and for identification of the various proteins interacting with ferric siderophores during iron uptake (*39*, *40*). It requires the use of a photoactivatable but chemically inert ligand analogue, which generates a highly reactive species on illumination that binds irreversibly to the biological receptor at the site of interaction. The labeled amino acid is then identified by sequencing. The photoactivatable functional group used here was aryl azide. Aryl azides are chemically inert in the dark but produce extremely reactive aryl nitrenes on photolysis. These compounds form stable bonds with most types of compounds (*41*) and are sufficiently reactive to insert even into C−H bonds.

The sites chosen for the binding of the photoactivatable group on PvdI were the succinyl moiety linked to C-3 of the chromophore for $N_3$-Chromo−PvdI-Fe, as described previously ((*35*); Figure 2) and the hydroxyl group of Ser1 of the peptide for $N_3$-Ser−PvdI-Fe (Figure 2). All coupling reactions with the 4-azidobenzoic acid *N*-hydroxysuccinimide ester and the siderophore were performed on the ferric complex of the siderophore. This prevented side reactions at other sites on the siderophore, such as the reactive catechol and hydroxamate groups. We synthesized $N_3$-Ser−PvdI-Fe by mixing PvdI-Fe(III) with an excess of 4-azidobenzoic acid *N*-hydroxysuccinimide ester in the presence of triethylamine. One major product was obtained after purification. Two-dimensional NMR spectra of the free ligand (TOCSY, $^1$H-$^{13}$C HMQC, and $^1$H-$^{13}$C HMBC spectra) were recorded. This enabled us to assign all resonances and to demonstrate that the arylazido moiety was bound to the Ser1 residue. Only the chemical shift of Ser1 differed from what was observed

for PvdI (*31*) (chemical shift of CO-**C**H-NH, PvdI, 63.98 ppm; $N_3$-Ser−PvdI, 66.5 ppm). For $N_3$-Chromo−PvdI-Fe, a nucleophilic amino group was introduced on the succinyl arm as described previously (*35*), except that the iron-loaded form of the aminopyoverdine was used to prevent side reactions at other sites on the siderophore. In a previous study, we used the iron-free form (*35*) and at least three secondary products were obtained according to mass spectrometry analysis of the reaction mixture. The reactive catechol or hydroxamate groups may have reacted with the 4-azidobenzoic acid *N*-hydroxysuccinimide ester. In this study, the arylazido group was introduced in the amino derivative of PvdI-Fe(III) using only 1.2 equiv of 4-azidobenzoic acid *N*-hydroxysuccinimide ester and not an excess as for the synthesis of $N_3$-Ser−PvdI-Fe. One major product was observed after purification. The $^1$H and $^{13}$C chemical shifts of the amino acids were identical to those determined for $NH_2$-PvdI (*31*). However, three new correlations were found by HMBC, confirming the presence of the arylazido group bound to the chomophore of PvdI ($^2J$ correlation between the N***H*** group of ethylenediamine (8.38 ppm) and the ***C***O (172.48); $^3J$ correlation between C$\boldsymbol{H}_2$ of ethylenediamine (3.64 ppm) and ***C***O (172.48); $^3J$ correlation between C***H*** of arylazido (7.64 ppm) and ***C***O (172.48)).

Pflu, the siderophore produced by *P. fluorescens*, is able to transport iron in *P. aeruginosa* ATCC 15692. We therefore used this siderophore to synthesize a third photoactivatable analogue of PvdI, $N_3$-Lys−Pflu-Fe. Pflu differs slightly from PvdI in terms of its peptide moiety (Figure 2). Some amino acids, including Ser1 and the two $\delta$*N*-hydroxyornithine residues involved in iron chelation are common to both molecules (*5*, *6*, *13*, *31*). Lysine and formyl hydroxyornithine are present in the peptide macrocycles of both pyoverdines, but in Pflu, L-Ser replaces the L-Thr−L-Thr pair of PvdI. For the synthesis of $N_3$-Lys−Pflu-Fe, the photoactivatable functional group was bound to the Lys $\epsilon$-amino group of the Pflu-Fe peptide moiety (Figure 2) by mixing Pflu-Fe with 1.2 equiv of 4-azidobenzoic acid *N*-hydroxysuccinimide ester, in the presence of triethylamine. The major product was purified by HPLC. The presence of the arylazido group on the Lys $\epsilon$-amino group was confirmed by the appearance of a peptidic H$\epsilon$ resonance in the spin system of the Lys residue in the TOCSY spectrum of $N_3$-Lys−Pflu-Fe (no such resonance was observed in the spectrum of unmodified Pflu). Furthermore, the H$\delta$ resonances of the Lys residue were shifted downfield by almost 0.6 ppm with respect to unmodified Pflu.

*Reversible Binding to Purified FpvAI.* The specificity of iron uptake in gram-negative bacteria is regulated by OMTs. These OMTs are highly specific for one or a small number of siderophores. We investigated the specificity of FpvAI for PvdI-Fe in more detail by determining the binding constants of the PvdI photoactivatable analogues from equilibrium competition experiments, as described previously (*19*), in vitro (using purified FpvAI) and in vivo (using PvdI-deficient CDC5(pPVR2) cells placed at 0 °C to prevent uptake). For the photoactivatable PvdI analogues, these experiments were carried out in the dark, so that these molecules were stable ($t_{1/2}$ > 24 h). Iron-free and iron-loaded $N_3$-Chromo−PvdI and $N_3$-Ser−PvdI have affinities for FpvAI in vivo and in vitro similar to that of the natural PvdI (Table 1). This suggests that the coupling of an arylazido to Ser1 or the succinyl moiety linked to C-3 of the chromophore (Figure 2) does not affect the properties of PvdI binding to FpvAI. PvdI and Pflu displayed very similar binding affinities for FpvAI in vitro and in vivo, whether loaded with iron or iron-free (Table 1). Thus, the differences in structure of the cyclic peptide moieties of PvdI and Pflu (Figure 2) and the replacement of the Arg in PvdI by a Lys in Pflu have no effect on the binding properties of the siderophore (Table 1). However, steric hindrance of the Lys residue of the peptide moiety of $N_3$-Lys−Pflu-Fe and $N_3$-Lys−Pflu significantly decreased affinity for FpvAI both in vitro and in vivo (Table 1). In this case, the coupling of an arylazido group to this basic residue disrupted the interaction between FpvAI and its siderophore, in both the presence and absence of iron. The differences in structure between PvdI and the three photoactivatable analogues had similar effects on affinity for FpvAI, for the iron loaded and the iron-free forms. This observation suggests that PvdI and PvdI-Fe interact with the binding site of FpvAI via the same mechanism.

Table 1: Inhibition Constants ($K_i$) of PvdI and Pflu Analogues for Purified FpvAI and for FpvAI Overproduced in CDC5(pPVR2) Cells[a]

| siderophores | $K_i$ (nM) purified FpvAI ($n = 3$) | $K_i$ (nM) CDC5(pPVR2) ($n = 3$) |
|---|---|---|
| PvdI-Fe | 7.5 ± 3 | 2.3 ± 2.3 |
| PvdI | 17.0 ± 1.5 | 12.0 ± 2 |
| $N_3$-Ser−PvdI-Fe | 3.0 ± 0.6 | 2.4 ± 0.6 |
| $N_3$-Ser−PvdI | 16.5 ± 0.5 | 4.8 ± 0.8 |
| $N_3$-Chromo−PvdI-Fe | 11.0 ± 1 | 3.4 ± 0.8 |
| $N_3$-Chromo−PvdI | 19.1 ± 0.1 | 5.2 ± 1.5 |
| Pflu-Fe | 19.0 ± 3 | 6.5 ± 0.9 |
| Pflu | 31.0 ± 2.3 | 19.8 ± 2.2 |
| $N_3$-Lys−Pflu-Fe | 388 ± 4 | 315 ± 5 |
| $N_3$-Lys−Pflu | 423 ± 14 | 495 ± 20 |

[a] The $K_i$ values were determined in competition experiments against PvdI-$^{55}$Fe. CDC5(pPVR2) cells ($OD_{600}$ of 0.05) or purified FpvAI receptors (1 nM) were incubated in the dark, in the presence of 1 nM and 12 nM PvdI-[$^{55}$Fe], respectively, and various concentrations of siderophore analogues. For $K_i$ determination in vivo, the cells were incubated at 0 °C to prevent iron uptake.

*Iron Transport Properties of PvdI Analogues.* The iron uptake efficiency of the PvdI photoactivatable analogues was estimated in *P. aeruginosa* ATCC 15692, using $^{55}$Fe (*19*). $N_3$-Chromo−PvdI-$^{55}$Fe and $N_3$-Ser−PvdI-$^{55}$Fe transport iron as efficiently as PvdI-$^{55}$Fe. Continuous irradiation at 312 nm during $^{55}$Fe uptake had no effect on iron uptake: no inhibition of uptake due to irreversible labeling of the PvdI-Fe binding site on FpvAI by the photoactivatable probe was observed. We previously described a similar experiment, carried out under irradiation, for $N_3$-Chromo−PvdI-$^{55}$Fe, in which iron uptake decreased by 15% (*35*). This decrease was an artifact resulting from the method used to synthesize iron-free $N_3$-Chromo−PvdI (complexed with $^{55}$Fe; see the description of the synthesis of $N_3$-Chromo−PvdI-Fe above). The protocol used by Ocaktan et al. (*35*) for the synthesis of iron-free $N_3$-Chromo−PvdI leads to the formation of secondary products, which certainly have a lower affinity for iron. Ocaktan et al. complexed $N_3$-Chromo−PvdI with $^{55}$Fe without further purification. All the analogues of PvdI studied here were purified by HPLC and characterized by NMR and mass spectrometry. Iron uptake data for $N_3$-Chromo−PvdI-$^{55}$Fe and $N_3$-Ser−PvdI-$^{55}$Fe showed that C-3 of the chro-

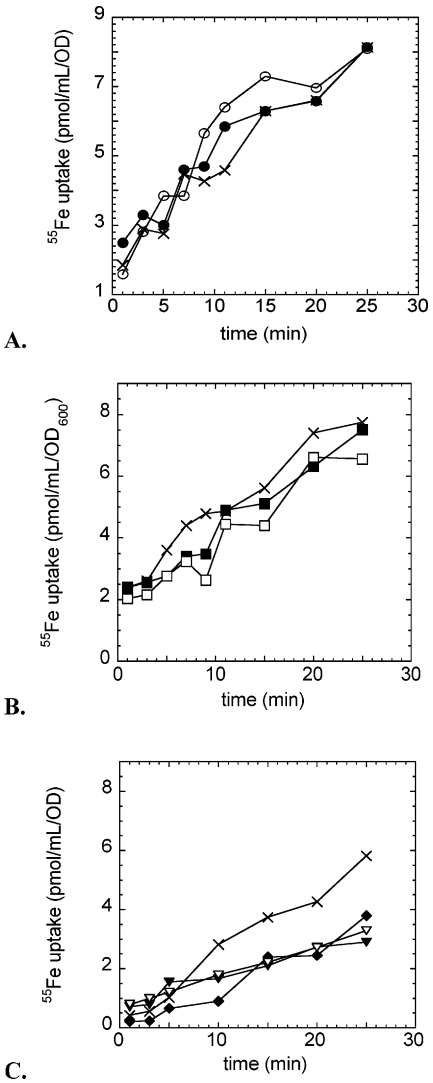


FIGURE 3: $^{55}$Fe uptake by *P. aeruginosa*. *P. aeruginosa* ATCC 15692 cells at a concentration of $1.3 \times 10^9$ cfu/mL were incubated for 15 min in the dark, in 900 $\mu$L of 50 mM Tris-HCl, pH 8.0, before the beginning of the transport assays. After this incubation, (A) 100 $\mu$L of PvdI-$^{55}$Fe (×) or $N_3$-Chromo−PvdI-$^{55}$Fe (●, in the dark), prepared as previously described (*35*), was added to the cells. The experiment was repeated for $N_3$-Chromo−PvdI-$^{55}$Fe (○) under irradiation at 312 nm; (B) 100 $\mu$L of PvdI-$^{55}$Fe (×) or $N_3$-Ser−PvdI-$^{55}$Fe (■, in the dark) was added to the cells and the experiment repeated for $N_3$-Ser−PvdI-$^{55}$Fe (□) under irradiation at 312 nm; and (C) 100 $\mu$L of PvdI-$^{55}$Fe (×) Pflu-$^{55}$Fe (◆) or $N_3$-Lys−Pflu-$^{55}$Fe (▼, in the dark) was added to the cells. The experiment was repeated for $N_3$-Lys−Pflu-$^{55}$Fe (▽) under irradiation at 312 nm. For each run, 100 $\mu$L aliquots were removed at various time points, filtered, and counted. The kinetics studies presented in each panel were carried out in parallel on the same batch of cells, always with PvdI-$^{55}$Fe as a reference. Data shown are not the averages of multiple experiments, but experiments were repeated at least three times. The three panels show a difference in iron uptake rates by a factor of 2 for PvdI-$^{55}$Fe. These differences may be due to differences in FpvAI expression or in the batches of *P. aeruginosa* ATCC 15692 used.

mophore and Ser1 of the peptide moiety were sterically hindered by a cumbersome succinyl moiety without disrupting iron uptake by the siderophore.

Pflu transports $^{55}$Fe in *P. aeruginosa* but less efficiently than PvdI (35% less efficient, Figure 3C). This difference was significant and confirms the findings of Hohnadel and Meyer (*5*). The structural differences between Pflu and PvdI (see Figure 2) are important for iron transport. If the Lys residue of the peptide moiety of Pflu-$^{55}$Fe is sterically hindered by an arylazido group ($N_3$-Lys−Pflu-$^{55}$Fe), the rate of iron uptake is unaffected and remains similar to that for Pflu-$^{55}$Fe (Figure 3C). Under irradiation at 312 nm, no inhibition of $^{55}$Fe incorporation into *P. aeruginosa* cells was observed with $N_3$-Lys−Pflu-$^{55}$Fe.

These findings confirm that the structural differences between PvdI-Fe and Pflu-Fe have an impact on iron uptake rates in *P. aeruginosa* ATCC 15692 cells. However, modification of the siderophores by a cumbersome arylazido group at three different positions in PvdI or Pflu ($N_3$-Chromo−PvdI-$^{55}$Fe, $N_3$-Ser−PvdI-$^{55}$Fe, and $N_3$-Lys−Pflu-$^{55}$Fe) surprisingly had no effect on the iron uptake process.

*Iron Uptake and PvdI Recycling Monitored by FRET.* We used FRET between PvdI and the Trp residues of the proteins to follow PvdI-Fe uptake in *P. aeruginosa*. As described previously, when *P. aeruginosa* cells are incubated in the presence of low concentrations of PvdI-Fe (ratio 1−5 PvdI-Fe equivalent for one FpvAI), a typical fluorescent signal is obtained (*38*). This signal is characterized first by a decrease of fluorescence corresponding to the formation of FpvA−PvdI-Fe for most of the FpvAI−PvdI complexes present at the cell surfaces. The second step is an increase of fluorescence corresponding to the recycling of the iron-free PvdI on the FpvAI transporter, after iron release (Figure 4). This signal was observed for Pflu-Fe and for the three photoactivatable analogues of PvdI-Fe (Figure 4), demonstrating that these molecules complete the iron uptake cycle, forming FpvAI−siderophore-Fe complexes (decrease of fluorescence, due to the exchange of siderophore on FpvA−Pvd (*20*, *38*)), releasing the iron, and recycling the iron-free analogue on FpvAI (increase in fluorescence, (*38*)). Continuous irradiation of the sample at 290 nm (excitation of the Trp), leading to photodecomposition of the probes and possible irreversible labeling of the transporter, seemed to have no effect on iron uptake with the PvdI analogues. A difference in the amplitude of the fluorescent signal was observed, especially for $N_3$-Chromo−PvdI-Fe and $N_3$-Lys−Pflu-Fe, due to a change in the fluorescence properties of these molecules (data not shown). The spectral properties of these molecules seem to be modulated by the chemical modification. The coupling of a cumbersome arylazido group to PvdI-Fe would be expected to slow the uptake process or, at least, the recycling of iron-free siderophore on FpvA. Surprisingly, neither of these two steps were slowed for $N_3$-Chromo−PvdI-Fe and $N_3$-Ser−PvdI-Fe. For $N_3$-Lys−Pflu-Fe, recycling seemed to be slightly slower than for PvdI-Fe or Pflu-Fe (Figure 4).

*Analysis of the Labeled FpvAI Receptor in Vivo and in Vitro.* $N_3$-Chromo−PvdI-Fe, $N_3$-Ser−PvdI-Fe, and $N_3$-Lys−Pflu-Fe are photoactivatable analogues of PvdI and were designed for the labeling of FpvAI and of any protein in the periplasm, inner membrane, or cytoplasm involved in the Pvd-Fe uptake process. Half-lives deduced from photodecomposition of the three photoactivatable analogues, with and without iron loading, in 50 mM Tris-HCl (pH 8.0) buffer, were between 7 and 10 min (data not shown), consistent with the iron uptake kinetics (Figures 3 and 4). PvdI-deficient CDC5(PPVR2) cells were incubated under irradiation at 312 nm in the presence of the various tritiated photoactivatable analogues of PvdI or Pflu, with and without iron loading. The same experiment was repeated for each probe in the

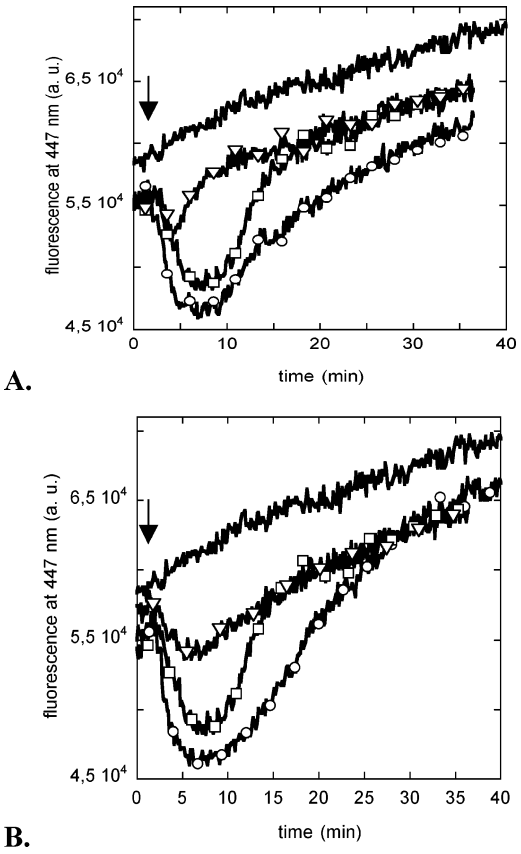


FIGURE 4: Iron uptake monitored by FRET. PvdI-producing, FpvAI-overproducing K691(pPVR2) cells at an $OD_{600}$ of 0.7 were incubated in 50 mM Tris-HCl (pH 8.0) at 29 °C. After the addition of 100 nM PvdI-Fe (□, panels A and B), $N_3$-Chromo−PvdI-Fe (▽, panel A), $N_3$-Ser−PvdI-Fe (○, panel A), Pflu-Fe (○, panel, B), and $N_3$-Lys−Pflu-Fe (▽, panel B), changes in fluorescence at 447 nm (excitation set at 290 nm) were monitored by measuring fluorescence emission at 447 nm. The experiment was repeated in the absence of ferric siderophore (black line, panels A and B).

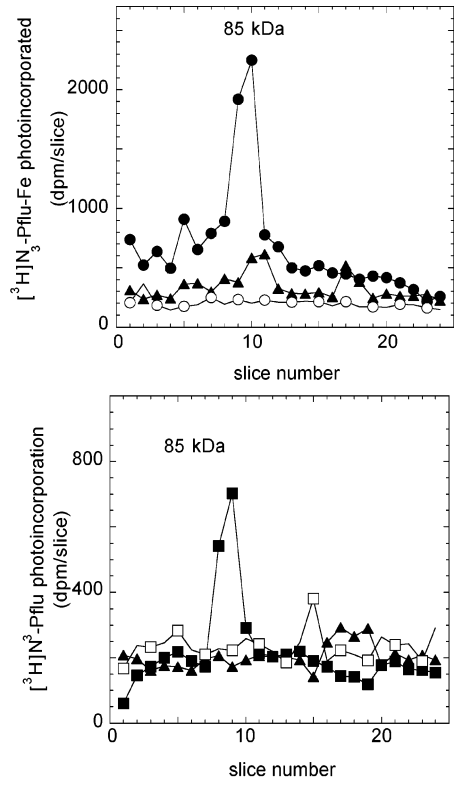


FIGURE 5: Photoaffinity labeling of FpvAI by [$^3$H]$N_3$-Lys−Pflu-Fe and [$^3$H]$N_3$-Lys−Pflu (A) In vivo photoaffinity labeling of FpvAI by iron-loaded [$^3$H]$N_3$-Lys−Pflu. CDC5(pPVR2) cells at an $OD_{600}$ of 1.6 were incubated under irradiation at 312 nm in the presence of 120 $\mu$M [$^3$H]$N_3$-Lys−Pflu-Fe alone (●), or with 1 mM PvdI-Fe as a protective agent (○) in 50 mM Tris-HCl, pH 8.0. The experiment was repeated with no irradiation and no protective agent (▲). After irradiation, the outer membranes were isolated for each mixture, as described in Materials and Methods, and labeling was analyzed by SDS−PAGE. (B) In vivo photoaffinity labeling of FpvAI by iron-free [$^3$H]$N_3$-Lys−Pflu. The experiment described in panel A was repeated with iron-free [$^3$H]$N_3$-Lys−Pflu as the photoactivatable probe and PvdI as the protective agent. Experiments were carried out in the presence of [$^3$H]$N_3$-Lys−Pflu under irradiation (■) and in the absence of irradiation (▲) and in the presence of PvdI and irradiation (□).

presence of excess PvdI-Fe, to saturate the siderophore-binding site and to determine labeling specificity. Labeling reactions were also carried out in the dark, to demonstrate that the observed labeling of the protein was induced photochemically. The cells were then lysed, the various cell compartments were separated, and the labeling was analyzed for each compartment by SDS−PAGE. For $N_3$-Lys−Pflu-Fe and $N_3$-Lys−Pflu, a peak of radioactivity was observed in the outer membranes only under irradiation, in the slices corresponding to the migration of FpvAI (band at 85 kDa, Figure 5). In competition experiments, with irradiation in the presence of the photoactivatable analogue of PvdI plus an excess of PvdI-Fe or iron-free PvdI, the radioactive peak was abolished in the presence of PvdI-Fe during irradiation. Thus, labeling involved the specific binding site for PvdI-Fe on FpvAI. Similar results were obtained for $N_3$-Chromo−PvdI-$^{55}$Fe and $N_3$-Ser−PvdI-$^{55}$Fe (results not shown). Unfortunately, labeling percentages were very low in all cases: less than 1% for iron-loaded and iron-free $N_3$-Chromo−PvdI and $N_3$-Se−-PvdI and around 3% for $N_3$-Lys−Pflu-Fe and $N_3$-Lys−Pflu. We carried out similar experiments with purified FpvAI, but the rate of labeling of the FpvAI transporter was no higher (data not shown). We analyzed the other cell compartments, periplasm, inner membrane, and cytoplasm, by SDS−PAGE, but no labeling was observed for the ferric form of the three photoactivatable analogues. The rate of labeling may have been too low to be observed. Alternatively, the ferric PvdI analogues may not have interacted with proteins in the periplasm, inner membrane, or cytoplasm.

## DISCUSSION

The OMTs of pseudomonads involved in iron uptake via Pvds are usually highly specific and able to transport only the Pvd produced by the strain itself. This specificity is probably governed by the specificity of the OMT binding site. The molecular interactions involved in the recognition of Pvds by their specific OMTs have been studied mostly for FpvAI from *P. aeruginosa* ATCC 15692 and its siderophore PvdI. PvdI and PvdI-Fe bind to a common or overlapping binding site on FpvAI, with a 10-fold difference in affinity in favor of PvdI-Fe (*19*, *20*, *22*). In both cases, binding occurs in two steps, but with much slower kinetics for the iron-free form than for the iron-loaded form of PvdI (*22*). Time-resolved fluorescence spectroscopy studies have shown that there are two different conformations of FpvAI−PvdI, depending on the method of preparation used (formed

in vitro or in vivo prior to purification). When formed in vivo, the dihydroquinoline moiety of the siderophore is not as flexible and solvent-accessible and its environment is not as polar as that of FpvAI−PvdI formed in vitro (*42*). In the presence of metal ions, the solvent accessibility and mobility of the dihydroquinoline moiety are intermediate between those for the two metal-free conformations. Moreover, in FpvAI−PvdI formed in vitro, three Trp residues are involved in the FRET with PvdI, whereas two Trp residues are involved in FpvAI−PvdI and FpvAI−PvdI-metal complexes (*42*). These time-resolved fluorescence spectroscopy data demonstrate that there are at least two conformations for FpvAI−PvdI. Only the structure of the in vivo FpvAI−PvdI complex has been resolved (*16*). This complex has a hydrophobic binding site for PvdI, composed of six Tyr, three Trp, three Gln, one Asn, one Val, one Gly, and one Arg residue. PvdI-metal competes with apo-PvdI for this binding site (*19*, *22*). The in vivo FpvAI−PvdI complex is only stable in the pH range 4−8.5 (Figure 1A). The binding of PvdI and PvdI-metal to FpvA was optimal at pH 8.0 (Figure 1B). At pH values exceeding 8.5, one or several binding site residues may become ionized, disrupting the FpvAI−PvdI complex or inhibiting the formation of FpvAI−PvdI or FpvAI−PvdI-metal complexes. The six Tyr residues and the two Arg residues in the PvdI binding site may become ionized at pH values exceeding 8. These residues have a p$K_a$ in solution of 10.07 (Tyr) and 12.48 (Arg) (the precise values depend on the environment of the amino acid).

In FpvAI−PvdI (*16*), PvdI is attached to the plug domain via the chromophore, which is common to all Pvds. Ser1 and Arg of the peptide moiety fold around the chromophore and the rest of the peptide folds over the chromophore (Figure 6A). The peptide moiety, which determines the specificity of each Pvd, interacts mainly with the $\beta$-barrel domain and the extracellular loops rather than with the plug domain (*16*). When an arylazido group is coupled to the succinyl moiety linked to C-3 of the chromophore of PvdI or PvdI-metal or to Ser2, affinity for FpvAI is unaffected (Table 1). Less than 1% of FpvAI transporters were labeled in the presence of these two probes in photolabeling experiments. These data reflect the nonprotein environment of the arylazido group of these two molecules in the FpvAI binding site. The aryl nitrenes formed after irradiation may therefore be rapidly quenched by the surrounding water molecules. In the FpvAI−PvdI structure (*16*), the succinyl moiety points to the $\beta$-barrel and faces the $\beta$-strands $\beta$17 and $\beta$18 and the extracellular loop L9 (Figure 6B). L9 is a short loop, generating a gap between loop L8 and L10 (Figure 6B,D). The arylazido group linked to the succinyl moiety can fold toward the extracellular site in this large gap between loop L8 and L10 (Figure 6B,D). In FpvAI−PvdI, Ser1 is sandwiched between $Tyr_{600}$ and $Trp_{599}$ and points slightly toward the extracellular site (Figure 6C,A). In FpvAI−$N_3$-Ser−PvdI, with and without iron loading, the arylazido group must fold over $Tyr_{600}$ and $Trp_{599}$ in the gap and points toward the extracellular site (Figure 6D,E), without having a major effect on the positioning of the rest of the siderophore in its binding site.

Pflu and PvdI, with and without iron loading, have similar $K_i$ for FpvAI in vitro and in vivo (Table 1). Pflu probably sits in the FpvAI binding site with a conformation similar to that of PvdI in FpvA−PvdI (*16*). The structural differences between PvdI and Pflu (Figure 2) are not important for the interaction of the siderophore with FpvAI. The coupling of the arylazido group to the Lys of Pflu ($N_3$-Lys−Pflu) decreased the $K_i$ of the apo and ferric forms of the siderophore for FpvAI in vivo by factors of 48 and 25 (Table 1). There is generally a basic residue in the second position of the peptide moiety in Pvds (*43*). In FpvAI−PvdI, the Lys of PvdI (residue equivalent to Arg in Pflu) points toward the plug domain (Figure 6A), interacts with $D_{597}$ of loop L7 (Figure 6C), and is covered by part of loop L7 (Figure 6D,F). In accordance with the structure of FpvAI−PvdI, the Arg residue of PvdI cannot be subject to steric hindrance due to an arylazido group without a major effect on the position of the siderophore in its binding site and a decrease in affinity (Figure 6D,F). Only about 3% of FpvAI was labeled with the iron-loaded or iron-free $N_3$-Lys−Pflu. In FpvAI−$N_3$-Lys−Pflu-Fe and FpvAI−$N_3$-Lys−Pflu, the arylazido group is probably forced to point toward the extracellular site because of a lack of space between the Lys of Pflu and the $\beta$-barrel of FpvAI. This probably disrupts the interaction of the siderophore with L7. In this case, surrounding water might rapidly quench the photoinduced aryl nitrenes.

The pH of the environment and the chemical modifications to PvdI (coupling of an arylazido group) have similar effects on the binding of PvdI and PvdI-Fe to FpvA. This suggests that PvdI and PvdI-Fe have similar mechanisms of recognition and interaction with FpvAI but with different binding kinetics (*22*). The conformation of PvdI-metal probably fits perfectly into the FpvAI binding site, accounting for its rapid binding. Apo-PvdI can exist in various conformations and has to adapt its conformation to the binding site. It therefore binds more slowly to FpvAI. These data suggest that it is the kinetics of siderophore−receptor binding that are important in Fe transport, rather than the thermodynamics ($K_i$). However, time-resolved fluorescent spectroscopy studies have shown that the change of conformation induced on FpvAI by the binding of PvdI depends on the loading status of the siderophore (*42*). Therefore, we cannot exclude that only the binding of PvdI-Fe induces an essential change of conformation on FpvAI necessary for the uptake process.

Once the FpvAI receptor is loaded with ferric PvdI, the TonB machinery located in the inner membrane activates the receptor, leading to transport of the ferric PvdI by an unknown mechanism. It appears unlikely, in terms of thermodynamics, that the plug domain of the OMT is removed and floats freely in the periplasm during transport of the ferric siderophore. The plug is held in place by numerous hydrogen bonds and polar contacts with the barrel interior. Nevertheless, as noted by Faraldo-Gomez and coworkers (*44*), comparable numbers of H-bonds can be found in some dissociation complexes such as tRNA synthetases and their tRNAs. Molecular dynamics experiments have shown that extensive solvation of the barrel−plug interface by relative localized water molecules occurs in FhuA (the ferrichrome outer membrane transporter in *E. coli*). On the basis of these observations, it has been proposed that water molecules facilitate dissociation of the two domains, or at least induction of a conformational change sufficient to allow the formation of a channel between the barrel and the plug, for permeation of the ligand. In a mechanism such as this, in which the ferric-siderophore has to worm its way through the FpvAI structure between the plug and the $\beta$-barrel

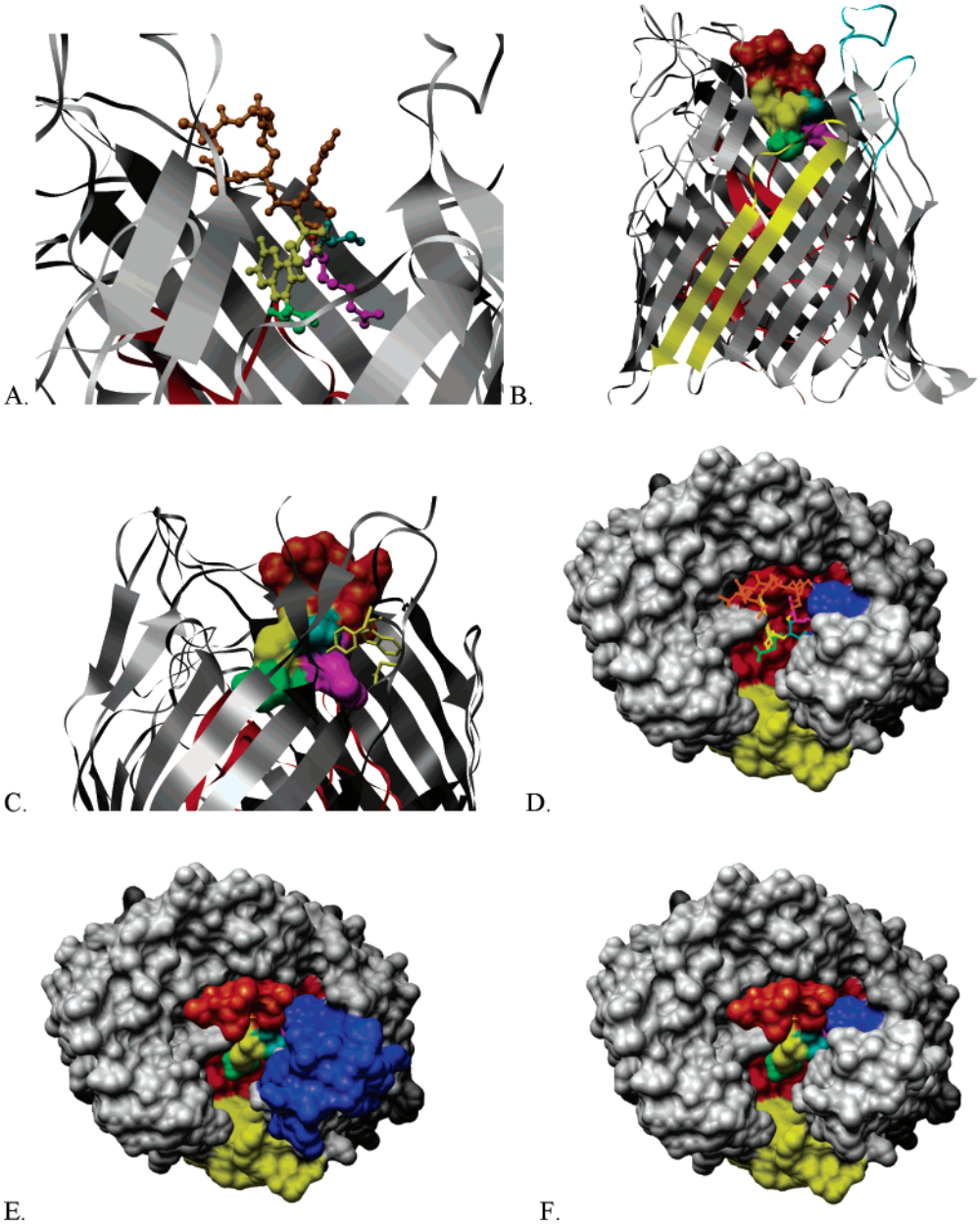


FIGURE 6: FpvAI−PvdI structure (*16*). In A−F, the chromophore of PvdI is shown in yellow, the succinyl part in green, Ser1 in cyan, Arg in magenta, and the rest of the peptide in brown. FpvAI is drawn as a ribbon for panels A−C and as a space-filling representation for panels D−F. The $\beta$-barrel domain is shown in gray in each case, and the plug domain in red. For panels A−C, view of the receptor is perpendicular to the $\beta$-barrel axis. For panels D−F, view is along the $\beta$-barrel axis. (A) PvdI is represented in its binding site on FpvAI. (B) The figure shows how the succinyl part (in green) of PvdI points to L9. L9 and the $\beta$-strands $\beta$18 and $\beta$19 are shown in yellow. (C) The figure shows how the Arg (in purple) of PvdI interacts with $D_{597}$ (stick representation in yellow) and Ser1 (in cyan) with $T_{600}$ and $W_{599}$ (stick representation in yellow) of L7. (D) Stick representation of PvdI and space-filling representation of FpvAI along the $\beta$-barrel axis. L9 and the $\beta$-strands $\beta$18 and $\beta$19 are shown in yellow and $T_{600}$ and $W_{599}$ of L7 in blue. (E) Space-filling representation of PvdI and of FpvAI along the $\beta$-barrel axis. L9 and the $\beta$-strands $\beta$18 and $\beta$19 are shown in yellow and L7 and L8 in blue. (F) Same representation of FpvAI−PvdI as in panel D, except that PvdI is shown as a space-filling representation.

domain, we would have expected siderophore-Fe uptake to have been slower with the three photoactivatable probes ($N_3$-Chromo−PvdI−Fe, $N_3$-Ser−PvdI-Fe, and $N_3$-Lys−Pflu-Fe), as an arylazido group linked to PvdI would be cumbersome. Surprisingly, no decrease in iron uptake efficiency was observed for the three photoactivatable probes (Figures 3 and 4). Moreover, after iron release, the photoactivatable analogues of PvdI were recycled as efficiently as natural PvdI (increase in fluorescence, Figure 4). In a mechanism in which the photoactivatable analogues must interact with several different proteins, for iron uptake (OMT, periplasmic binding protein, ABC transporter) and then for siderophore recycling (transporters involved in the siderophore recycling), the presence of a cumbersome arylazido group on PvdI would have been expected to slow at least one of these steps considerably, affecting the FRET signal. For the mechanism of ferric siderophore uptake through the outer membrane, all these data are more consistent with a mechanism involving release of the plug from the $\beta$-barrel domain of FpvAI, followed by the dissociation of iron from the siderophore in the periplasm. Another mechanism consistent with our data is release of the iron from the siderophore on the FpvAI receptor, with translocation of the iron ion but not of the ferric siderophore into the periplasm. This mechanism is

similar to that of iron uptake from transferrin by TonB-dependent OMTs (*45*). In both cases, the mechanism of iron uptake via PvdI in *P. aeruginosa* would be different from that of ferrichrome or enterobactin in *E. coli*, in which the ferric siderophore is transported through the outer and inner membranes by an OMT and an ABC transporter, respectively. Early studies of ferric pyoverdine uptake, using radiolabeled PvdI (*46*) or Mössbauer spectroscopy (*47*), suggested that iron and PvdI dissociated in the periplasm but did not propose a mechanism. When incubated in the presence of [$^{14}$C]PvdI-$^{55}$Fe, iron-poor *P. aeruginosa* cells accumulated more $^{55}$Fe than $^{14}$C over a 60 min period. Cells osmotically shocked after this incubation, released $^{55}$Fe but not $^{14}$C, suggesting separation of metal and siderophore in the periplasm (*46*). Mössbauer spectroscopic investigation of PvdI-Fe uptake by *P. aeruginosa* revealed that no PvdI-Fe accumulates in the cells during incubation periods of 20, 40, 60, or 120 min (*47*). Moreover, the genomic sequence of *P. aeruginosa* lacks genes encoding periplasmic/cytoplasmic membrane transporters for the ferric siderophores used by this bacterium, but encodes large numbers of possible outer membrane receptors (32 putative OMTs, http://www.pseudomonas.com). This suggests that, in *P. aeruginosa*, iron is removed from most of the siderophores in the periplasm or at the outer membrane and that an iron-specific transporter delivers the metal to the cytoplasm. This would also account for the lack of protein labeling in the periplasm and inner membrane during iron uptake by the photoactivatable analogues of PvdI or Pflu. Iron release from the siderophore on FpvAI presumably involves a dissociation mechanism induced by the OMT itself and/or by the TonB machinery.

PvdI-$^{55}$Fe and Pflu-$^{55}$Fe have similar affinities for FpvAI (Table 1) but gave uptake rates differing by 35% (Figure 3C, (*5*)). The structural differences between PvdI and Pflu (Figure 2) reside in the replacement of Ser2 by a Gly, Arg by a Lys, and the pair of Thr residues by a single Ser residue. The replacement of Arg by Lys is a conservative modification as both residues are basic. The replacement of Ser2 by a Gly and of the pair of Thr residues by a single Ser, in the part of PvdI pointing to the extracellular medium, induces significant chemical modifications on the siderophore, which may account for the differences in behavior observed between PvdI and Pflu in $^{55}$Fe uptake. This part of the PvdI peptide must be more important for the interaction of the ferric siderophore with FpvAI during iron uptake than during binding. The binding site may be closed by some extracellular loop, as in FecA (*28*). In this OMT, loops L8 and L7 close over the ferric citrate and the transporter is in a conformation competent for iron uptake. L8 and L7 face PvdI in FpvAI (Figure 6E) and may undergo a conformational change, leading to interaction with the peptide moiety of Pvd during iron or ferric siderophore uptake. Consistent with this hypothesis, previous time-resolved fluorescence spectroscopy studies (*42*) have shown that, in the FpvAI−PvdI-metal complex, the PvdI is less mobile, less solvent accessible, and in a less polar environment than in the FpvAI−PvdI complex, suggesting that it may be trapped in its binding site due to conformational changes in some of the extracellular loops.

The low ABC transporter gene content of the *P. aeruginosa* ATCC 15692 genome, Mössbauer analysis of iron uptake (*47*), the distribution of radiolabeled PvdI after iron uptake (*46*), and the binding and iron uptake properties of the PvdI photoactivatable analogues presented here suggest a mechanism of iron uptake different from that described for ferrichrome or enterobactin in *E. coli*. In the PvdI iron uptake pathway, iron seems to dissociate from its siderophore on FpvAI or in the periplasm, close to the OMT.

## ACKNOWLEDGMENT

We thank our many collaborators who have contributed to this work by helpful discussions, including Dr. Jean-Jacques Bernardini and Dr. Franc Pattus.

## REFERENCES

1. Braun, V. (2003) Iron uptake by *Escherichia coli*, *Front. Biosci. 8*, s1409−1421.
2. Koster, W. (2001) ABC transporter-mediated uptake of iron, siderophores, heme and vitamin B12, *Res. Microbiol. 152*, 291−301.
3. Moeck, G. S., and Coulton, J. W. (1998) TonB-dependent iron acquisition: mechanisms of siderophore-mediated active transport, *Mol. Microbiol. 28*, 675−681.
4. Postle, K., and Kadner, R. J. (2003) Touch and go: tying TonB to transport, *Mol. Microbiol. 49*, 869−882.
5. Hohnadel, D., and Meyer, J. M. (1988) Specificity of pyoverdine-mediated iron uptake among fluorescent *Pseudomonas* strains, *J. Bacteriol. 170*, 4865−4873.
6. Budzikiewicz, H. (1993) Secondary metabolites from fluorescent pseudomonads, *FEMS Microbiol. Rev. 10*, 209−228.
7. Atkinson, R. A., Salah El Din, A. L., Kieffer, B., Lefevre, J. F., and Abdallah, M. A. (1998) Bacterial iron transport: $^{1}$H NMR determination of the three-dimensional structure of the gallium complex of pyoverdin G4R, the peptidic siderophore of *Pseudomonas putida* G4R, *Biochemistry 37*, 15965−15973.
8. Mohn, G., Koehl, P., Budzikiewicz, H., and Lefevre, J. F. (1994) Solution structure of pyoverdin GM-II, *Biochemistry 33*, 2843−2851.
9. Teintze, M., Hossain, M. B., Barnes, C. L., Leong, J., and van der Helm, D. (1981) Structure of ferric pseudobactin, a siderophore from a plant growth promoting *Pseudomonas*, *Biochemistry 20*, 6446−6457.
10. Marugg, J. D., de Weger, L. A., Nielander, H. B., Oorthuizen, M., Recourt, K., Lugtenberg, B., van der Hofstad, G. A., and Weisbeek, P. J. (1989) Cloning and characterization of a gene encoding an outer membrane protein required for siderophore-mediated uptake of $Fe^{3+}$ in *Pseudomonas putida* WCS358, *J. Bacteriol. 171*, 2819−2826.
11. O'Sullivan, D. J., Morris, J., and O'Gara, F. (1990) Identification of an additional ferric-siderophore uptake gene clustered with receptor, biosynthesis, and *fur*-like regulatory genes in fluorescent *Pseudomonas* sp. strain M114, *Appl. Environ. Microbiol. 56*, 2056−2064.
12. Meyer, J. M., Stintzi, A., De Vos, D., Cornelis, P., Tappe, R., Taraz, K., and Budzikiewicz, H. (1997) Use of siderophores to type pseudomonads: the three *Pseudomonas aeruginosa* pyoverdine systems, *Microbiology 143* (Pt 1), 35−43.
13. Meyer, J. M., Stintzi, A., and Poole, K. (1999) The ferripyoverdine receptor FpvA of *Pseudomonas aeruginosa* PAO1 recognizes the ferripyoverdines of *P. aeruginosa* PAO1 and *P. fluorescens* ATCC 13525, *FEMS Microbiol. Lett. 170*, 145−150.
14. Cornelis, P., Hohnadel, D., and Meyer, J. M. (1989) Evidence for different pyoverdine-mediated iron uptake systems among *Pseudomonas aeruginosa* strains, *Infect. Immun. 57*, 3491−3497.
15. Poole, K., Neshat, S., Krebes, K., and Heinrichs, D. E. (1993) Cloning and nucleotide sequence analysis of the ferripyoverdine receptor gene *fpvA* of *Pseudomonas aeruginosa*, *J. Bacteriol. 175*, 4597−4604.
16. Cobessi, D., Célia, H., Folschweiller, N., Schalk, I. J., Abdallah, M. A., and Pattus, F. (2005) The crystal structure of the pyoverdin outer membrane receptor FpvA from *Pseudomonas aeruginosa* at 3.6 Å resolution, *J. Mol. Biol. 347*, 121−134.
17. de Chial, M., Ghysels, B., Beatson, S. A., Geoffroy, V., Meyer, J. M., Pattery, T., Baysse, C., Chablain, P., Parsons, Y. N., Winstanley, C., Cordwell, S. J., and Cornelis, P. (2003) Identifica-

tion of type II and type III pyoverdine receptors from *Pseudomonas aeruginosa*, *Microbiology 149*, 821−831.
18. Ghysels, B., Dieu, B. T., Beatson, S. A., Pirnay, J. P., Ochsner, U. A., Vasil, M. L., and Cornelis, P. (2004) FpvB, an alternative type I ferripyoverdine receptor of *Pseudomonas aeruginosa*, *Microbiology 150*, 1671−1680.
19. Schalk, I. J., Kyslik, P., Prome, D., van Dorsselaer, A., Poole, K., Abdallah, M. A., and Pattus, F. (1999) Copurification of the FpvA ferric pyoverdin receptor of *Pseudomonas aeruginosa* with its iron-free ligand: implications for siderophore-mediated iron transport, *Biochemistry 38*, 9357−9365.
20. Schalk, I. J., Hennard, C., Dugave, C., Poole, K., Abdallah, M. A., and Pattus, F. (2001) Iron-free pyoverdin binds to its outer membrane receptor FpvA in *Pseudomonas aeruginosa*: a new mechanism for membrane iron transport, *Mol. Microbiol. 39*, 351−360.
21. Schalk, I. J., Yue, W. W., and Buchanan, S. K. (2004) Recognition of iron-free siderophores by TonB-dependent iron transports, *Mol. Microbiol. 54*, 14−22.
22. Clément, E., Mesini, P. J., Pattus, F., Abdallah, M. A., and Schalk, I. J. (2004) The binding mechanism of pyoverdin with the outer membrane receptor FpvA in *Pseudomonas aeruginosa* is dependent on its iron-loaded status, *Biochemistry 43*, 7954−7965.
23. Cobessi, D., Celia, H., and Pattus, F. (2005) Structure of ferric-pyochelin and its membrane receptor FptA from *Pseudomonas aeruginosa*, *J. Mol. Biol. 352*, 893−904.
24. Ferguson, A. D., Hofmann, E., Coulton, J. W., Diederichs, K., and Welte, W. (1998) Siderophore-mediated iron transport: crystal structure of FhuA with bound lipopolysaccharide, *Science 282*, 2215−2220.
25. Locher, K. P., Rees, B., Koebnik, R., Mitschler, A., Moulinier, L., Rosenbusch, J. P., and Moras, D. (1998) Transmembrane signaling across the ligand-gated FhuA receptor: crystal structures of free and ferrichrome-bound states reveal allosteric changes, *Cell 95*, 771−778.
26. Buchanan, S. K., Smith, B. S., Venkatramani, L., Xia, D., Esser, L., Palnitkar, M., Chakraborty, R., van der Helm, D., and Deisenhofer, J. (1999) Crystal structure of the outer membrane active transporter FepA from *Escherichia coli*, *Nat. Struct. Biol. 6*, 56−63.
27. Ferguson, A. D., Chakraborty, R., Smith, B. S., Esser, L., van der Helm, D., and Deisenhofer, J. (2002) Structural basis of gating by the outer membrane transporter FecA, *Science 295*, 1715−1719.
28. Yue, W. W., Grizot, S., and Buchanan, S. K. (2003) Structural evidence for iron-free citrate and ferric citrate binding to the TonB-dependent outer membrane transporter FecA, *J. Mol. Biol. 332*, 353−368.
29. Ankenbauer, R., Hanne, L. F., and Cox, C. D. (1986) Mapping of mutations in *Pseudomonas aeruginosa* defective in pyoverdin production, *J. Bacteriol. 167*, 7−11.
30. Wendenbaum, S., Demange, P., Dell, A., Meyer, J. M., and Abdallah, M. A. (1983) The structure of pyoverdin Pa, the siderophore of *Pseudomonas aeruginosa*, *Tetrahedron Lett. 24*, 4877−4880.
31. Demange, P., Wendenbaum, S., Linget, C., Mertz, C., Cung, M. T., Dell, A., and Abdallah, M. A. (1990) Bacterial siderophores: structure and NMR assigment of pyoverdins PaA, siderophores of *Pseudomonas aeruginosa* ATCC 15692, *Biol. Met. 3*, 155−170.
32. Linget, C., Azadi, P., MacLeod, J. K., Dell, A., and Abdallah, M. A. (1992) Bacterial siderophore: the structure of the pyoverdins of *Pseudomonas fluorescens* ATCC 13525, *Tetrahedron Lett. 33*, 1737−1740.
33. Demange, P., Abdallah, M. A., and Frank, H. (1988) Assignment of the configurations of the amino acids in peptidic siderophores, *J. Chromatogr. 438*, 291−297.
34. Albrecht-Garry, A. M., Blanc, S., Rochel, N., Ocacktan, A. Z., and Abdallah, M. A. (1994) Bacterial iron transport: coordination properties of pyoverdin PaA, a peptidic siderophore of *Pseudomonas aeruginosa*, *Inorg. Chem. 33*, 6391−6402.
35. Ocaktan, A., Schalk, I., Hennard, C., Linget-Morice, C., Kyslik, P., Smith, A. W., Lambert, P. A., and Abdallah, M. A. (1996) Specific photoaffinity labelling of a ferripyoverdin outer membrane receptor of *Pseudomonas aeruginosa*, *FEBS Lett. 396*, 243−247.
36. Mizuno, T., and Kageyama, M. (1978) Separation and characterization of the outer membrane of *Pseudomonas aeruginosa*, *J. Biochem. (Tokyo) 84*, 179−191.
37. Spratt, B. G. (1977) Properties of the penicillin-binding proteins of *Escherichia coli* K12, *Eur. J. Biochem. 72*, 341−352.
38. Schalk, I. J., Abdallah, M. A., and Pattus, F. (2002) Recycling of pyoverdin on the FpvA receptor after ferric pyoverdin uptake and dissociation in *Pseudomonas aeruginosa*, *Biochemistry 41*, 1663−1671.
39. Kotzyba-Hibert, F., Kapfer, I., and Goeldner, M. (1995) Recent trends in photoaffinity labeling, *Angew. Chem., Int. Ed. 34*, 1296−1312.
40. Grutter, T., Bertrand, S., Kotzyba-Hibert, F., Bertrand, D., and Goeldner, M. (2002) Structural reorganization of the acetylcholine binding site of the torpedo nicotinic receptor as revealed by dynamic photoaffinity labeling, *ChemBioChem 3*, 652−658.
41. Bayley, H., and Knowles, J. R. (1977) Photoaffinity labeling, *Methods Enzymol. 46*, 69−114.
42. Folschweiller, N., Gallay, J., Vincent, M., Abdallah, M. A., Pattus, F., and Schalk, I. J. (2002) The interaction between pyoverdin and its outer membrane receptor in *Pseudomonas aeruginosa* leads to different conformers: a time-resolved fluorescence study, *Biochemistry 41*, 14591−14601.
43. Abdallah, M. A., and Pattus, F. (2000) Siderophores and iron-transport in microorganisms, *J. Chin. Chem. Soc. 47*, 1−20.
44. Faraldo-Gomez, J. D., Smith, G. R., and Samson, M. S. P. (2003) Molecular dynamics simulations of the bacterial outer membrane protein FhuA: a comparative study of the ferrichrome-free and bound states, *Biophys. J. 85*, 1406−1420.
45. Clarke, T. E., Tari, L. W., and Vogel, H. J. (2001) Structural biology of bacterial iron uptake systems, *Curr. Top. Med. Chem. 1*, 7−30.
46. Royt, P. W. (1990) Pyoverdine-mediated iron transport. Fate of iron and ligand in *Pseudomonas aeruginosa*, *Biol. Met. 3*, 28−33.
47. Mielczarek, E. V., Royt, P. W., and Toth-Allen, J. (1990) A Mossbauer spectroscopy study of cellular acquisition of iron from pyoverdine by *Pseudomonas aeruginosa*, *Biol. Met. 3*, 34−38.

BI051155S